Journal of Mining and Earth Sciences

Website: http://tapchi.humg.edu.vn

Determination of Mud Weight for High Pore Pressure and High Temperature Wells in the Hai Thach Field, Vietnam

Phuong Viet Nguyen [1,*], Binh Thanh Bui [1]

[1] *Hanoi University of Mining and Geology, Vietnam*

ARTICLE INFO

Article history:
Received 12 Oct. 2016
Accepted 15 Mar. 2017
Available online 30 June 2017

Keywords:
HPHT
Hai Thach
Wellbore stability
Geomechanics
Mud weight window

ABSTRACT

Determination of suitable mud weights for the wells in the Hai Thach (HT-P) field is a very challenging task because of the high pore pressure and high temperature (HPHT) conditions. The main objective of this study is to determine a suitable mud weight for drilling into the HPHT zone of HT-P well. First, a thermo-chemo-pore-elastic model for calculating the stress around the wellbore is presented. Two failure criteria, Drucker-Prager and Mohr-Coulomb, are used and compared. Then, the determination of model inputs from well logs and available data is summarized. Finally, the numerical results of the model are analyzed to propose a new mud weight for the HPHT zone of HT-P well. The field data, modeling work and the proposed mud weight presented in this study can be used as a reference for drilling new wells in the Hai Thach field to avoid any wellbore instability problems.

1. Introduction

The Hai Thach field is located at Block 05-2, Nam Con Son basin, offshore Vietnam, approximately 330 km from Vung Tau (Figure 1). The average water depth is from 130 to 140 m. The bottomhole pressure is up to 11,500 psi (17.5 ppg), and formation temperature is up to 175°C at well the True Vertical Depth (TVD). The Hai Thach is considered as a high pressure and high temperature field. It was discovered in 1995 by BP with the gas and condensate accumulation in the Post-rift of the upper Miocene, the Syn-rift of the middle Miocene, and the lower Miocene (Figure 2 and Figure 3).

Wellbore instability is one of the major factors that significantly increases the cost and non-productive time in the Hai Thach field. The single most important cause of wellbore instability is the incorrect mud weight as depicted in Figure 4. The bottom-hole pressure, due to using high mud density, could be higher than the fracture gradient resulting in mud losses or wellbore fractures. On the other hand, too low mud weight can cause kick or borehole collapse. Thus, a safe mud weight window should be considered to ensure the safety and efficiency of the drilling process, especially for the wells with narrow mud weight windows such as wells in the Hai Thach field. A little change on mud density may have a great impact on wellbore stability. There were many difficulties and complexities in selecting optimum mud weight for the wells in the

*Corresponding author
E-mail: phuongnguyenviet94@gmail.com

Hai Thach field. The HT-P well experienced both fluid losses and gas influxes. When the well was drilled to 3000 mTVD with 17.1 ppg mud weight, kick occurred with 12% max gas. Therefore, the well was immediately shut in and monitored. The driller's method was used to kill the kick and the mud weight was then increased to 17.4 ppg. However, after raising the mud weight, the mud loss occurred at the rate of with 20 bbls per hour while circulating to clean the hole at the depth of 3053.6 mTVD. The mud losses and kicks occurred in a short drilling section are very challenging to resolve. To be able to continue drilling, it was decided to set a casing to seal this troubled interval. The above complex issues may be consequences of wellbore instability and always put the well in the dangerous situation. Therefore, wellbore stability analysis for the HT-P well in the Hai Thach field is essential to propose an optimum mud weight window for a successful drilling operation.

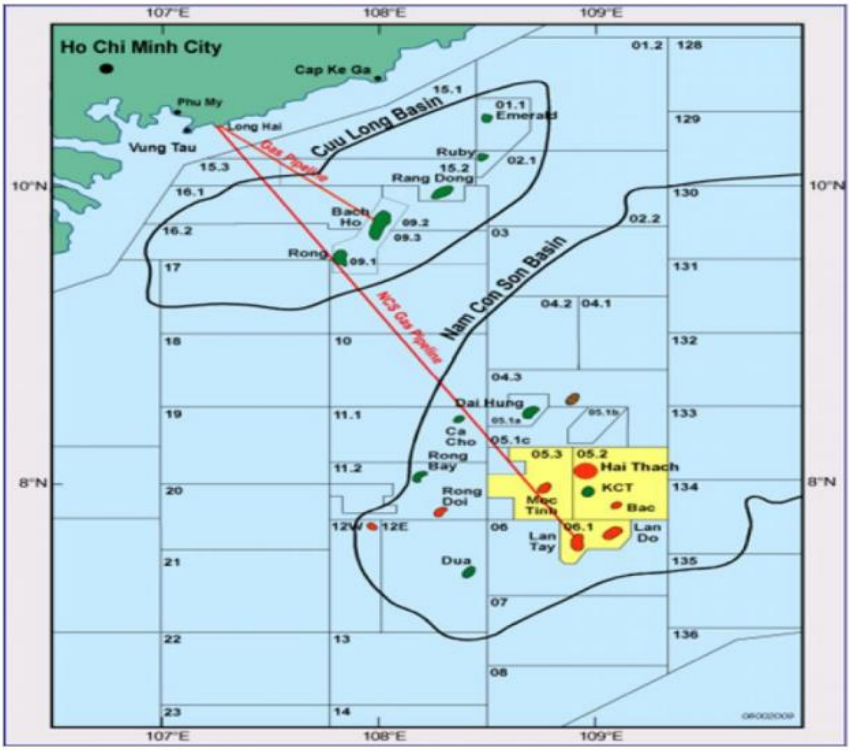

Figure 1. Location of the Hai Thach field offshore Vietnam (Nguyen et al., 2015).

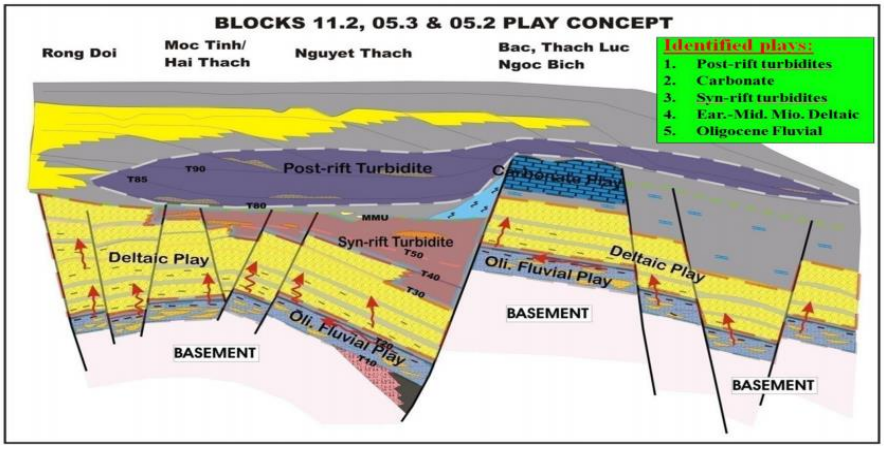

Figure 2. Play concept of blocks 05-2 and surrounding area (Nguyen et al., 2015).

2. Wellbore Stability Modeling

Stresses around the Wellbore

Stress concentration around the wellbore is generated by not only the alteration of the in-situ stresses but also temperature variation and chemical interaction. The effect and determination of these stresses can be found in published papers by (Wang, 1994; Ekbote and Abousleiman, 2005; Abousleiman, et al., 2013; Bui and Tutuncu, 2013). In this paper, the thermo-chemo-pore-elastic model accounted for the influence of temperature variation and chemical interaction was used for calculating the stress around the wellbore.

Before drilling, any point in the formation is subjected to an equilibrium state of stresses called in-situ stresses. The in-situ stresses are represented by three principal stresses consisting of a vertical stress σ_v due to the weight of the overlaying formations and fluids, and two horizontal stresses σ_H and σ_h created by the tectonic movements and the overburden. When a well is drilled in the formation, a stress concentration around the wellbore is created as a result of the alteration of in-situ stresses. This is the main reason causing wellbore instability. To find the stress state at each point at the wellbore wall, it is necessary to transform in-situ stresses in global coordinate system (x', y', z') to the cylindrically wellbore coordinate system (r, θ, z) by using an intermediate Cartesian coordinate system called the local coordinates (x, y, z), as shown in Figure 5.

In this study, Kirsch's equations (Kirsch, 1898) is used to determine the stress components around the borehole. Stresses in cylindrical coordinates are calculated as

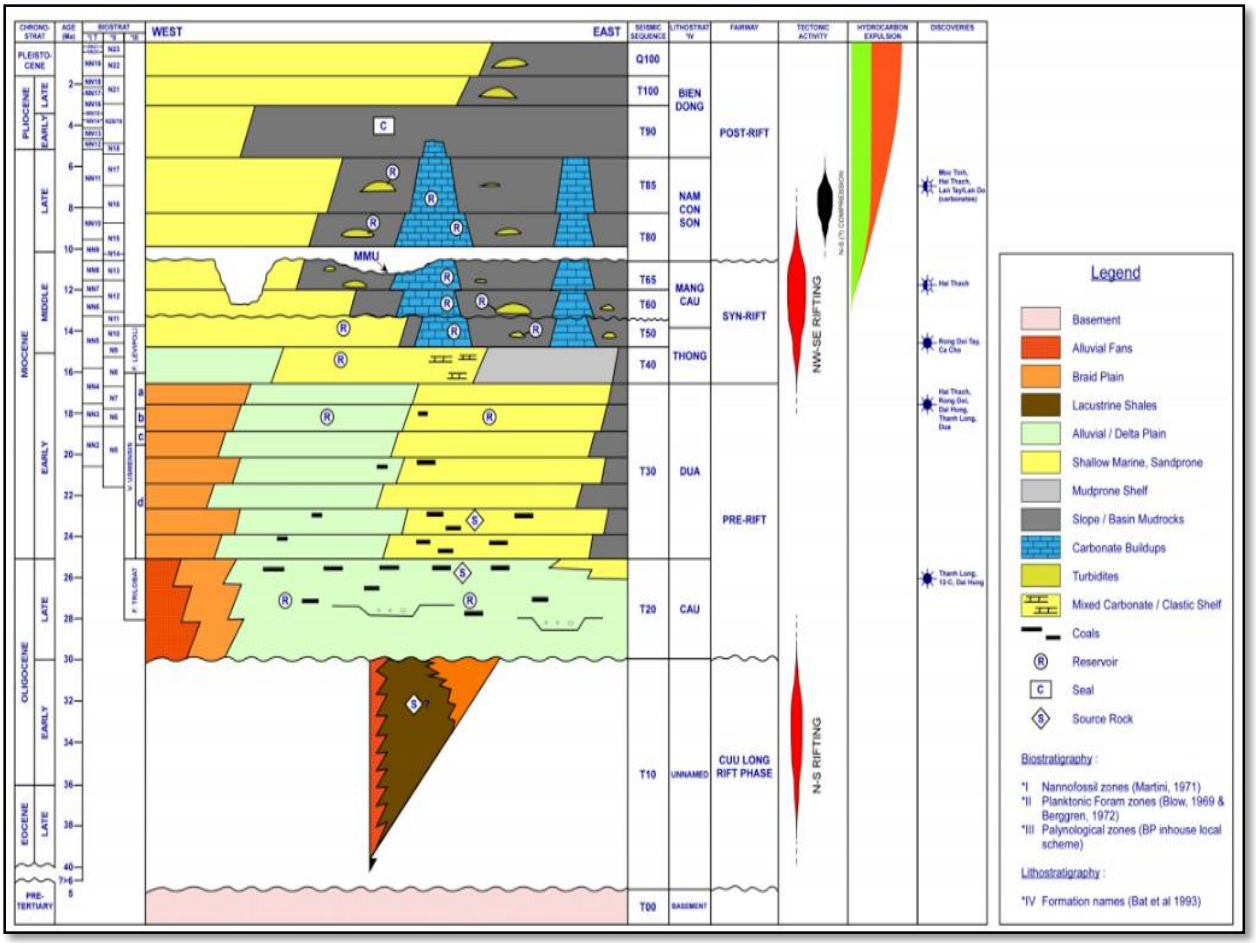

Figure 3. Nam Con Son Basin chronostratigraphic diagram (Nguyen et al., 2015).

Figure 4. Safe and stable mud weight windows (Rasouli, et al., 2010).

$$\sigma_r = \left(\frac{\sigma_{xx}+\sigma_{yy}}{2}\right)\left(1-\frac{r^2}{d^2}\right)+\left(\frac{\sigma_{xx}-\sigma_{yy}}{2}\right)\left(1+3\frac{r^4}{d^4}-4\frac{r^2}{d^2}\right)\cos 2\theta +$$
$$+\tau_{xy}\left(1+3\frac{r^4}{d^4}-4\frac{r^2}{d^2}\right)\sin 2\theta + p_w\frac{r^2}{d^2}$$
$$\sigma_\theta = \left(\frac{\sigma_{xx}+\sigma_{yy}}{2}\right)\left(1+\frac{r^2}{d^2}\right)-\left(\frac{\sigma_{xx}-\sigma_{yy}}{2}\right)\left(1+3\frac{r^4}{d^4}\right)\cos 2\theta +$$
$$-\tau_{xy}\left(1+3\frac{r^4}{d^4}\right)\sin 2\theta - p_w\frac{r^2}{d^2}$$
$$\sigma_z = \sigma_{zz}-\nu\left[2\left(\sigma_{xx}-\sigma_{yy}\right)\frac{r^2}{d^2}\cos 2\theta + 4\tau_{xy}\frac{r^2}{d^2}\sin 2\theta\right] \quad (1)$$
$$\tau_{r\theta} = \left(\frac{\sigma_{xx}-\sigma_{yy}}{2}\right)\left(1-3\frac{r^4}{d^4}+2\frac{r^2}{d^2}\right)\sin 2\theta +$$
$$+\tau_{xy}\left(1-3\frac{r^4}{d^4}+2\frac{r^2}{d^2}\right)\cos 2\theta$$
$$\tau_{\theta z} = \left(-\tau_{xz}\sin\theta+\tau_{yz}\cos\theta\right)\left(1+\frac{r^2}{d^2}\right)$$
$$\tau_{rz} = \left(\tau_{xz}\cos\theta+\tau_{yz}\sin\theta\right)\left(1-\frac{r^2}{d^2}\right)$$

where r is the wellbore radius, and d is the radial distance from wellbore axis. At the borewall, the equation above reduces to

$$\sigma_r = p_w$$
$$\sigma_\theta = \sigma_{xx}+\sigma_{yy}-2\left(\sigma_{xx}-\sigma_{yy}\right)\cos 2\theta - 4\tau_{xy}\sin 2\theta - p_w$$
$$\sigma_z = \sigma_{zz}-\nu[2(\sigma_{xx}-\sigma_{yy})\cos\theta + 4\tau_{xy}\sin 2\theta \quad (2)$$
$$\tau_{r\theta} = 0$$
$$\tau_{\theta z} = 2(-\tau_{xz}\sin\theta+\tau_{yz}\cos\theta)$$
$$\tau_{rz} = 0$$

where $\sigma_r, \sigma_\theta, \sigma_z$ are the radial stress, tangential stress and axial stress in the cylindrically wellbore coordinate system; $\tau_{r\theta}, \tau_{\theta z}, \tau_{rz}$ are three components of the shear stress in the cylindrically wellbore coordinate system; $\sigma_{xx}, \sigma_{yy}, \sigma_{zz}, \tau_{xy}, \tau_{yz}, \tau_{xz}$ are the stress components in the local coordinates; θ is the angle from the maximum horizontal stress; ν is Poisson's ratio; and p_w is the bottom hole pressure.

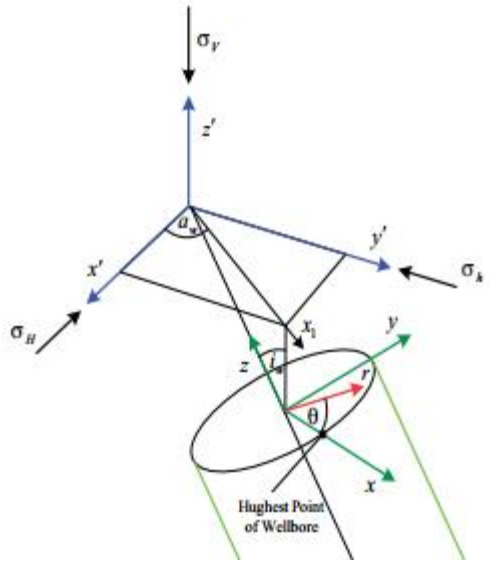

Figure 5. The coordinate system for the in-situ stress display (Pašić et al, 2007).

The stress components of the local coordinates can be expressed as,

$$\sigma_{xx} = \sigma_H\cos^2 A_w\cos^2 I + \sigma_h\cos^2 A_w\sin^2 I + \sigma_v\sin^2 A_w$$
$$\sigma_{yy} = \sigma_H\sin^2 A_w + \sigma_h\cos^2 A_w$$
$$\sigma_{zz} = \sigma_H\sin^2 A_w\cos^2 I + \sigma_h\sin^2 A_w\sin^2 I + \sigma_v\sin^2 A_w$$
$$\tau_{xy} = (\sigma_h-\sigma_H)\cos A_w\cos I\sin I \quad (3)$$
$$\tau_{yz} = (\sigma_h-\sigma_H)\sin A_w\cos I\sin I$$
$$\tau_{xz} = \sigma_H\cos A_w\sin A_w\cos^2 I +$$
$$+\sigma_h\cos A_w\sin A_w\sin^2 I - \sigma_v\sin A_w\cos A_w$$

where $\sigma_v, \sigma_H, \sigma_h$ are the vertical stress, maximum horizontal stress, and minimum horizontal stress, respectively; I is the inclination angle of borehole; A_w is the azimuth angle of borehole. To gain knowledge about the stress distribution surrounding the HT-P well, let's consider a zone of the wellbore and calculate the stress around the wellbore. In this paper, the selected zone is a troubled zone where the gas influx into the wellbore occurred. The input parameters to calculate the stress state at this zone are listed in Table 1.

Table 1. Data for determining the stress distribution around the HT-P well at 3000 mTVD.

Parameter	Value
TVD (m)	3000
Inclination Angle (deg.)	25
Azimuth Angle (deg.)	303
Young Modulus (psi)	2×10^6
Poisson's Ratio	0.18
Biot coefficients	1
Overburden Stress Gradient (ppg)	19.1
Pore Pressure Gradient (ppg)	17.56
Maximum Horizontal Stress Gradient (ppg)	19.21
Minimum Horizontal Stress Gradient (ppg)	18.41
Maximum Horizontal Stress Direction(deg.)	103

The stress distribution around the wellbore is shown in Figure 6 and Figure 7. It is observed that the radial stress σ_r at the wellbore wall is constant and independent of θ. Its value is equal of bottom-hole pressure. The radial and tangential stresses at the wellbore wall vary as a function of azimuth and radius. Both radial and tangential stresses reach the maximum value at the orientation of the minimum horizontal stress, ($\theta = 13°$ and $\theta = 193°$) and reach the minimum value at the orientation of the maximum horizontal stress ($\theta = 103°$ and $\theta = 283°$).

Chemical-induced stress

An osmotic pressure due to a difference in chemical activity between drilling fluid and water in formation generates a flow of water in or out of formation. These results in a significant pore pressure variation and can lead to rock strength weakening or failure due to stress disturbance around the wellbore. The flow direction is controlled by the salinity (ion type and concentration) of the fluid because water moves from the low solute concentration region (high chemical activity) to the high solute concentration region (low chemical activity).

The numerical equations for the osmotic pressure and its effect on the effective stresses acting at the wellbore wall are calculated as follows (Bui and Tutuncu, 2013):

$$\begin{aligned} s_r^c &= 0 \\ s_q^c &= a\frac{1-2n}{1-n}DP \\ s_z^c &= a\frac{1-2n}{1-n}DP \end{aligned} \quad (4)$$

where $\sigma_r^C, \sigma_\theta^C, \sigma_z^C$ are the alteration of radial, hoop and axial stresses due to the osmotic pressure, respectively; α is the Biot coefficient; ν is the Poisson's ratio, and $\Delta\Pi$ is the osmotic pressure. The osmotic pressure is calculated as

$$DP = -l_m\left(\frac{RT_O}{V_w}\right)ln\frac{a_{df}}{a_{sh}} \quad (5)$$

where l_m is the membrane coefficient, R is the universal gas constant and equals 8.314 J/K.mol; T_o is the absolute temperature; V_w is the molar volume of the water and equals 18.104 ml; a_{df}, a_{sh} are chemical activities of the drilling fluid and shale pore water, respectively.

Thermal-induced stress

The difference of temperature between drilling fluid and formation significantly influences the state of stress around wellbore. It is thus necessary to consider thermal effect on conducting a wellbore stability analysis, particularly in a HPHT environment like the Hai Thach field. Raising the temperature of the mud may lead to an increase in tangential stress, which enhances the likelihood of breakouts and inhibits tensile fracture. On the other hand, cooling the mud may leads to breakouts, which increases the likelihood of tensile fractures (Akong et al, 2011). The thermal induced stress can be calculated using the following equation (Bui and Tutuncu, 2013):

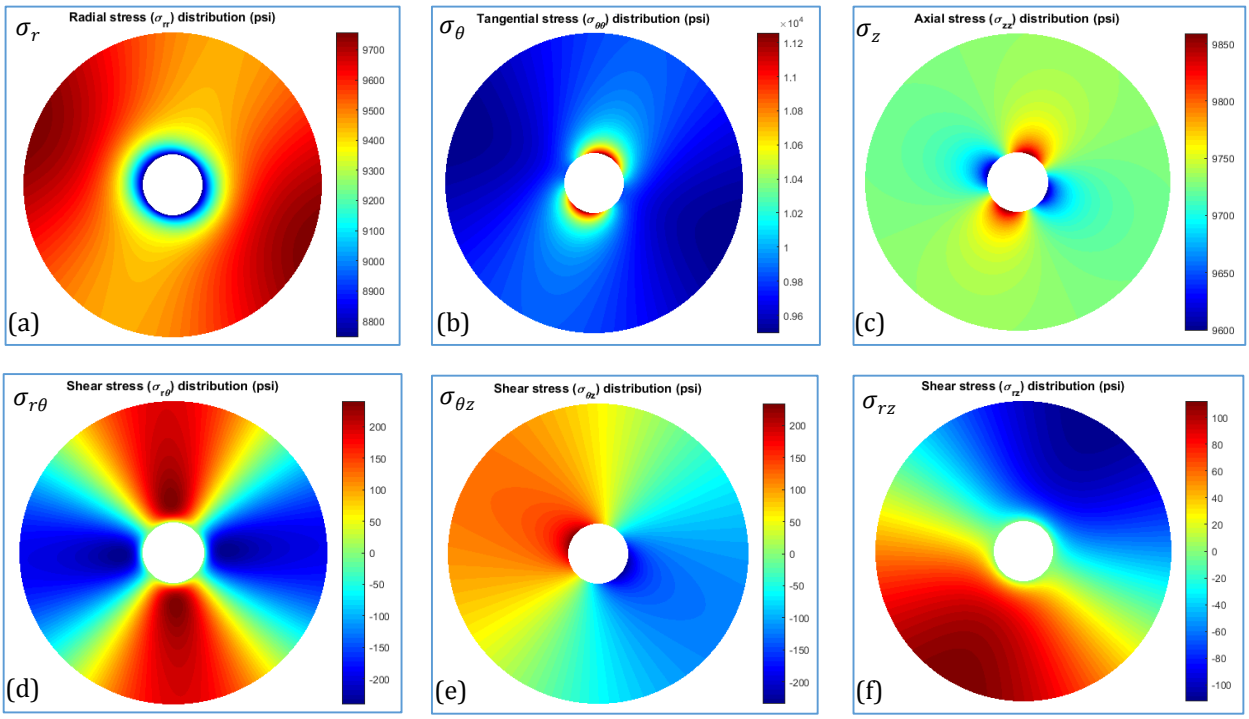

Figure 6. The variation of the stress surrounding the HT-P well at 3000 mTVD.

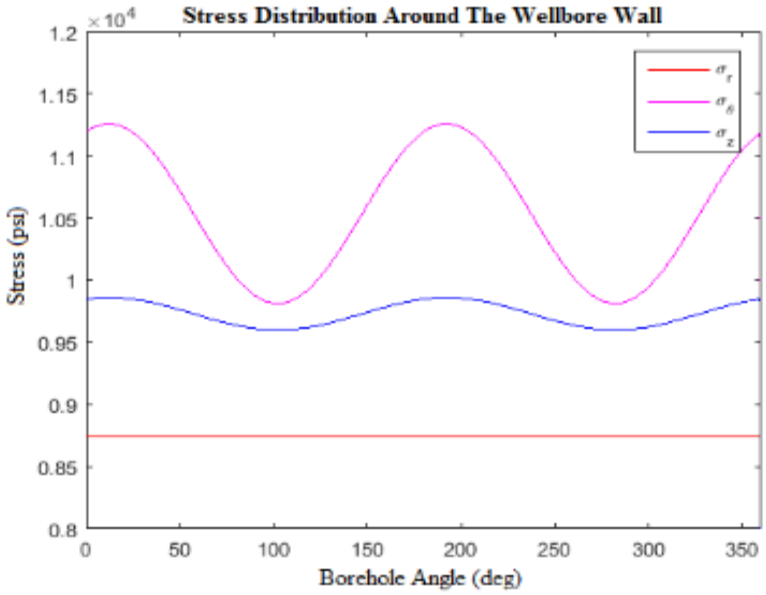

Figure 7. The variation of the stress at the wellbore wall of the HT-P well at 3000 mTVD.

$$s_r^T = 0$$
$$s_q^T = \frac{a_m E(T - T_O)}{1 - n} \quad (6)$$
$$s_z^T = \frac{a_m E(T - T_O)}{1 - n}$$

where $\sigma_r^T, \sigma_\theta^T, \sigma_z^T$ are the alteration of radial, hoop and axial stresses due to the thermal induced stress, respectively; ν is the Poisson's ratio; E is Young modulus; a_m is the volumetric thermal expansion coefficient of rock matrix; T is the circulation temperature; and T_o is the formation temperature.

The equations in the thermo-chemo-pore-elastic model that includes the effects of in-situ stresses, chemical interaction, and temperature

alteration to determine the stress concentration at the wellbore wall can be expressed as follows:

$$\begin{aligned}
&\sigma_r = p_w \\
&\sigma_\theta = \sigma_{xx} + \sigma_{yy} - 2\left(\sigma_{xx} - \sigma_{yy}\right)\cos 2\theta - \\
&- 4\tau_{xy}\sin 2\theta - p_w + \alpha\frac{1-2\nu}{1-\nu}\Delta\Pi + \frac{a_m E(T-T_o)}{1-\nu} \\
&\sigma_z = \sigma_{zz} - \nu[2(\sigma_{xx} - \sigma_{yy})\cos\theta + 4\tau_{xy}\sin 2\theta + \\
&+ \alpha\frac{1-2\nu}{1-\nu}\Delta\Pi + \frac{a_m E(T-T_o)}{1-\nu} \\
&\tau_{r\theta} = 0 \\
&\tau_{\theta z} = 2(-\tau_{xz}\sin\theta + \tau_{yz}\cos\theta) \\
&\tau_{rz} = 0
\end{aligned} \tag{7}$$

The principal stresses acting at the wall of a deviated well are calculated using Equation 8:

$$\begin{aligned}
s_1 &= s_r \\
s_2 &= \frac{s_q + s_z}{2} + \sqrt{\left(\frac{s_q - s_z}{2}\right)^2 + t_{qz}^2} \\
s_3 &= \frac{s_q + s_z}{2} - \sqrt{\left(\frac{s_q - s_z}{2}\right)^2 + t_{qz}^2}
\end{aligned} \tag{8}$$

Rock Failure Criteria

One of the main factors of wellbore stability analysis is the selection of a suitable rock failure criterion. There are many failure criteria such as Mohr-Coulomb criterion, Hoek-Brown criterion, Drucker-Prager criterion, Mogi-Coulomb criterion, and Von Mises criterion. In this paper, to calculate the minimum mud weight, two most common failure criteria, Drucker-Prager and Mohr-Coulomb, are used and compared. While the maximum mud weight is obtained by utilizing the tensile failure criterion.

Compressive Failure Criterion

A wellbore will fall in compressive failure if mud weight is insufficient to reduce the shear stress. This failure is also known as wellbore collapse or shear failure and controlled by increasing mud weight.

According to the Mohr-Coulomb criterion, compressional failure occurs when

$$c.\cos j + \sin j.s_m^{eff} - t_{max} \le 0 \tag{9}$$

where φ is the angle of internal friction; c is the rock cohesion; and τ_{max} and σ_m^{eff} are the maximum shear stress and the effective mean stress. These stresses are calculated from minimum and maximum principal stresses as

$$\begin{aligned}
s_m^{eff} &= \frac{s_{max} + s_{min}}{2} - p_p \\
t_{max} &= \frac{s_{max} - s_{min}}{2}
\end{aligned} \tag{10}$$

The Drucker-Prager criterion considers all three principal stresses and compressional failure occurs when

$$A + 3BJ_1^{eff} - \sqrt{J_2} \ge 0 \tag{11}$$

where J_1^{eff} and J_2 are the octahedral effective normal and shear stresses defined by

$$\begin{aligned}
J_1^{eff} &= \frac{s_1 + s_2 + s_3}{3} - p_p \\
J_2 &= \frac{\left(s_1 - s_2\right)^2 + \left(s_2 - s_3\right)^2 + \left(s_3 - s_1\right)^2}{6}
\end{aligned} \tag{12}$$

and A and B are rock constants. They depend on the angle of internal friction (φ) and the cohesion of rock *(c)* and are defined by

$$\begin{aligned}
A &= \frac{6c.\cos j}{\sqrt{3}(3 - \sin j)} \\
B &= \frac{2\sin j}{\sqrt{3}(3 - \sin j)}
\end{aligned} \tag{13}$$

Tensile Failure Criterion

Tensile failure occurs when the effective minimum principal stress at the bore wall reaches or exceeds the formation rock tensile strength. Therefore, the tensile failure criterion can be expressed as:

$$s_{min}^{eff} = s_{min} - p_p \ge |s_t| \tag{14}$$

where σ_{min}^{eff} is the effective minimum principal stress; and σ_t is the tensile strength of rock.

3. Determination of mud weight for HT-P well

The troubled zone of HT-P well is from 2900 mTVD to 3972 mTVD due to high temperature and high pore pressure. Drilling in this zone encountered challenges related to wellbore instability such as kick at 3000 mTVD and mud losses at 3053.6 mTVD. Therefore, a case study is conducted for this section. In this case study, we outline the determination of the input parameters for the wellbore stability model from well log data and laboratory measurements and recommend

a new mud weight program for HP-P well.

Input Data Determination

Magnitude of Overburden Stress

Overburden stress, also called vertical stress, was generated by the combined weight of the overburdens. Thus, it can be calculated by the following equation:

$$s_v = r_w g z_w + g \int_{z_w}^{z} r(z)\, dz \qquad (15)$$

where $\rho(z)$ is the formation bulk density, which is a function of depth and obtained from density logs; ρ_w is the density of seawater; z is the depth of the calculated point; z_w is the water depth; and g is the gravitational acceleration.

The overburden stress gradient S_v of HT-P well, which equals the overburden stress σ_v divided by TVD, is shown in Figure 8.

Pore Pressure

Calculating pore pressure is extremely important to determine mud weight window in the HPHT condition of the Hai Thach field. In this study, the Eaton's empirical equations (Eaton, 1972, 1975) are used to estimate pore pressure from resistivity and sonic logs. The profile of pore pressure is shown in Figure 8.

$$PP = S_v - (S_v - PP_n)\left(\frac{R_o}{R_n}\right)^n$$
$$PP = S_v - (S_v - PP_n)\left(\frac{\Delta t_n}{\Delta t}\right)^n \qquad (16)$$

where p_p is the formation pore pressure gradient; S_v is the overburden stress gradient; PP_n is the normal (hydrostatic) pore pressure gradient; R_o and Δt are the resistivity and sonic transit time obtained from well logging; R_n and Δt_n are the resistivity and sonic transit time at the normal (hydrostatic) pressure; n is the Eaton exponent.

Minimum Horizontal Stress

In this paper, the Eaton's method is also utilized to calculate magnitude of the minimum horizontal stress (Eq. 16) and Extended Leak-off Tests (XLOTs) data of the HT-P is utilized for calibration.

$$s_h = \frac{n}{1-n}\left(s_v - a p_p\right) + a p_p \qquad (17)$$

Magnitude and Orientation of Maximum Horizontal Stress

In this study, data obtained from XLOTs is also used to calculate the magnitude of the maximum horizontal stress. The results show that the order of stress magnitudes is $\sigma_H > \sigma_v > \sigma_h$. In other words, the stress regime is strike-slip.

Orientation of the maximum horizontal stress is determined using available FMI log data from three exploration wells in the Hai Thach field. According to Hoang et al. (2016), the direction of σ_H is 103±9°N, as shown in Figure 9.

Rock elastic coefficients

Dynamic rock elastic properties (Young's modulus and Poisson's Ratio) were obtained using sonic measurements providing shear and

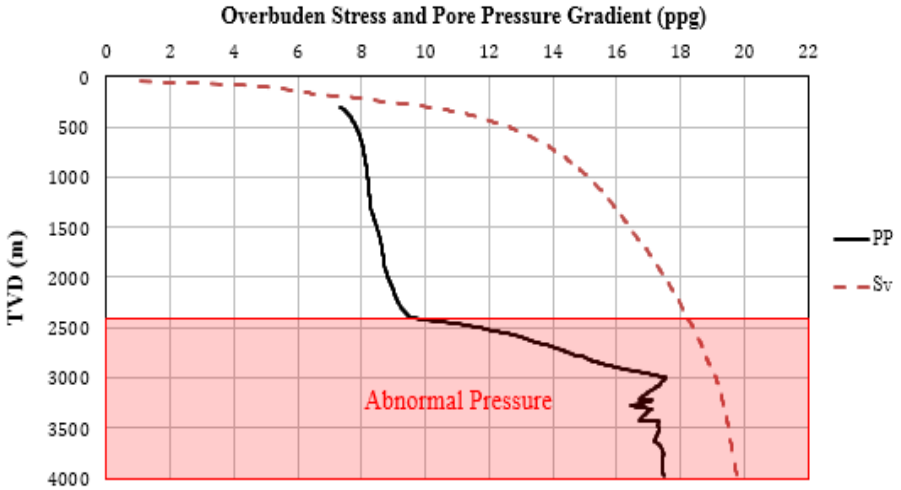

Figure 8. Overburden stress and pore pressure gradient profiles of the HT-P well.

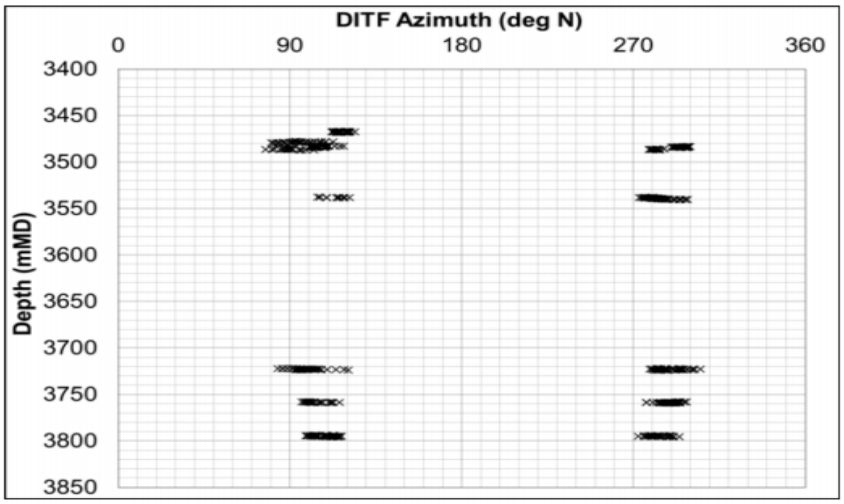

Figure 9. Profile of azimuth of drilling-induced tensile fractures (Hoang et al., 2016).

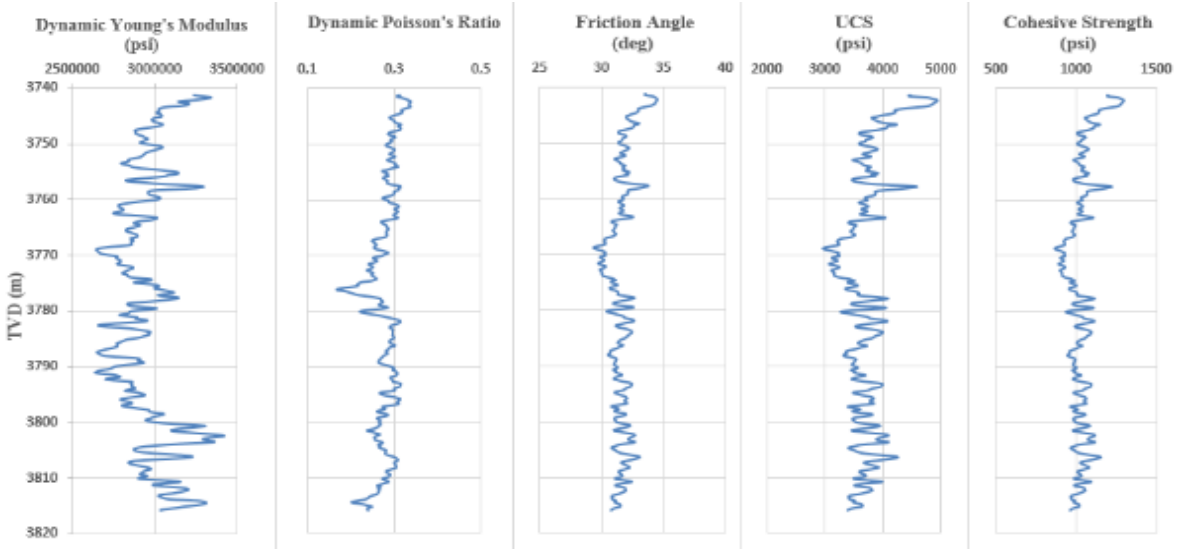

Figure 10. Formation geomechanical properties.

compressional slowness estimated from well log data. The results of the calculations are shown in Figure 10.

Dynamic Young's modulus:

$$E_d = \frac{r v_s^2 \left(3v_p^2 - 4v_s^2\right)}{v_p^2 - v_s^2} \quad (18)$$

Dynamic Poisson's ratio:

$$v_d = \frac{v_p^2 - 2v_s^2}{2(v_p^2 - v_s^2)} \quad (19)$$

where ρ is the bulk density; v_p is the compressional velocity; and v_s is the shear velocity.

The rock elastic data used for wellbore stability analysis are static data obtained from laboratory measurements. So, it is necessary convert dynamic data into static data. Dynamic Poisson's Ratio approximates the static value. However, there is a considerable difference between dynamic and static Young's modulus due to the variation in strain and strain rate. This paper uses the correlation proposed by Eissa and Kazi (1988) to determine the static Young's modulus from dynamic modulus. That correlation is written as

$$\log E_s = e + 0.77 \log(r E_d) \quad (20)$$

where e is the coefficient dependent on the rock porosity.

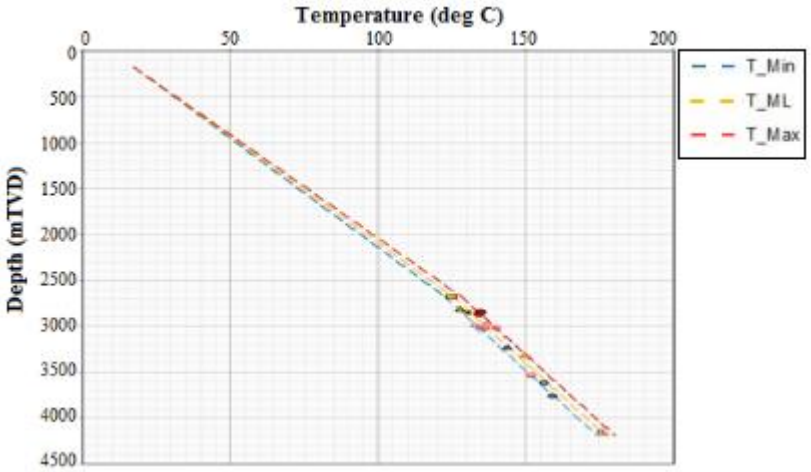

Figure 11. Temperature profile of the Hai Thach field (Hoang et al., 2016).

Table 2. The chemical activities of the drilling fluid and pore water.

Drilling section (mTVD)	Salinity of drilling fluid at 65°C (%)	Chemical activity of drilling fluid	Assumed salinity of pore water (%)	Chemical activity of pore water
2,900 ÷ 3,545	21.77 ÷ 23.84	0.83 ÷ 0.85	2.6	0.98
3,545 ÷ 3,972	22.52 ÷ 25.45	0.8 ÷ 0.84		

Rock strength

Typically, rock strength is obtained from laboratory core measurements. However, there is no available core measurement. Hence, in this study, the log and correlations (Equations 21-23) are used to determine the strength of rock in formation. The results of the calculations are shown in Figure 10.

Internal friction angle:

$$\varphi = \arcsin\frac{v_p - 1000}{v_p + 1000} \quad (21)$$

Unconfined Compressive Strength (UCS):

$$UCS = \frac{1}{k_1(\Delta t_p - k_2)^{k_3}} + k_4 \quad (22)$$

Rock cohesive strength:

$$c = UCS.\frac{1-\sin\varphi}{2\cos\varphi} \quad (23)$$

where v_p is the compressional velocity; Δt_p is the compressional slowness; and k_1, k_2, k_3, k_4 are lithology dependent coefficients.

In common practice, the tensile strength of rocks is negligible so it is considered to be zero in this study.

Thermal data

The HT-P well is considered as a HPHT well with bottom-hole temperature up to 175 deg C. Temperature profile of the Hai Thach field is shown in Figure 11. According to the End of Well Report of the HT-P well, the difference in temperature of the drilling fluid and virgin formation is 15°C. The rock thermal expansion coefficient in Equation 6 is linear thermal expansion that equals the volumetric thermal expansion coefficient divided by three (Huotari et al., 2004). Due to lack of laboratory measurements, in this study, this parameter was obtained from previous studies. In the study by Hoang et al. (2016), volumetric thermal expansion coefficient of rock in this zone is 3×10^{-5} °C^{-1}. Hence, the linear thermal expansion coefficient is estimated about 1×10^{-5} °C $^{-1}$.

Chemical data

The parameters to calculate the chemical-induced stress consist of the membrane coefficient and the chemical activities of the drilling fluid and pore water. The membrane efficiency describes ability of formation to restrict the flow of ions into or out of the pore and is from 0 to 1. In the studied zone, rock permeability is

very low with high clay content, value of reflection coefficient, thus, was assumed as 0.1.

The chemical activities of the drilling fluid and pore water were calculated by that based on the salinity in pore fluid and mud (Table 2).

Results and Discussion

Input data listed in Table 3 were used in the numerical calculation to examine the variation of mud weight with inclination and azimuth angles.

Mud weight at 3000 mTVD

The mud weight used to drill this zone was 17.1 ppg. The calculated results (Figure 12) show the difference in predictions of two breakout criteria. The Mohr-Coulomb criterion predicts that the borehole will be collapsed because the mud weight is lower than 17.51 ppg. Nevertheless, the Drucker-Prager criterion predicts the borehole will be stable with 16.90 ppg. In fact, there was no borehole collapse observed during drilling in this zone with the mud weight lower than 17.51 ppg. Hence, the Mohr-Coulomb criterion overestimated breakout pressure gradient and may not applicable for HT-P well. In addition, the results also indicate that there is no tensile failure since the fracture pressure gradient is 18.27 ppg, which is higher than the used mud weight.

In this zone, pore pressure is abnormally high and gas influx into the HT-P well is the consequence of using an incorrect mud weight due to under-estimation of pore pressure. To prevent gas influx in to the well, increasing mud weight is required and a mud weight of 17.6 ppg is proposed.

Mud weight at 3053.6 mTVD

As shown in Figure 13, the model predicts that the borehole will be stable at 3,053.6 mTVD with the actual used mud weight (17.6 ppg). This mud weight is lower than fracture pressure gradient (18.31 ppg) and greater than the collapse pressure gradient predicted by the Mohr-Coulumb criterion (17.29 ppg) and the Drucker-Prager criterion (16.54 ppg). The causes of mud losses observed in this zone during hole cleaning were because of the borehole damage during the the XLOT and the excessive ECD (17.9 ppg).

Table 3. Data for wellbore stability analysis.

Parameter	Value	
TVD (m)	3000	3053.6
Inclination Angle(deg.)	25	25
Azimuth Angle(deg.)	303	303
Tensile Strength (psi)	0	0
Unconfined Compressive Strength (psi)	2.06×10^3	2.49×10^3
Young Modulus (psi)	2×10^6	2.04×10^6
Poisson's Ratio	0.18	0.17
Biot coefficient	1	1
Internal Friction Angle (deg.)	25.39	27.51
Overburden Stress Gradient (ppg)	19.1	19,16
Pore Pressure Gradient (ppg)	17.56	17.39
Maximum Horizontal Stress Gradient (ppg)	19.21	19.28
Minimum Horizontal Stress Gradient (ppg)	18.41	18.39
Maximum Horizontal Stress Direction (deg.)	103	103
Rock Thermal Expansion Coefficient ($°C^{-1}$)	1×10^{-5}	1×10^{-5}
Temperature Difference (T- T_o) (°C)	-15	-15
Membrane Coefficient	0.1	0.1
Pore Water Activity	0.98	0.98
Drilling Fluid Activity	0.85	0.85
Formation Temperature (°C)	136	138

A new mud weight program for HT-P well

Repeating the determination of the mud weight for every depth in the "trouble" zone (2900 mTVD to 3930 mTVD), we obtain the mud weight window for this zone as shown in Figure 14. A new mud weight of 17.6 ppg is proposed to drill this section safely. Since the mud weight is quite narrow, accurate calculation of pressure surge and swap should be conducted to avoid any excessive variation of the mud weight.

Mud weight for deviated wells in the HPHT zone

In the previous section, a new mud weight program was proposed for HT-P well. In this section, we discuss the variation of the mud weight with the inclination and azimuth angles. The suitable mud weight not only depends on the depth but also does vary with the inclination and azimuth angles. For each pair of inclination and azimuth angles, a new mud weight should be determined.

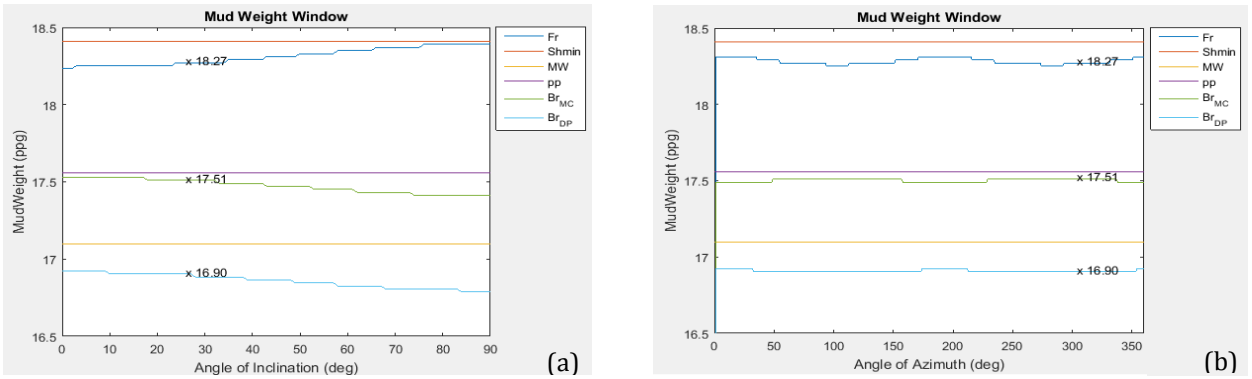

Figure 12. The variation of mud weight as a function of the inclination (a) and azimuth, (b) at 3,000 mTVD.

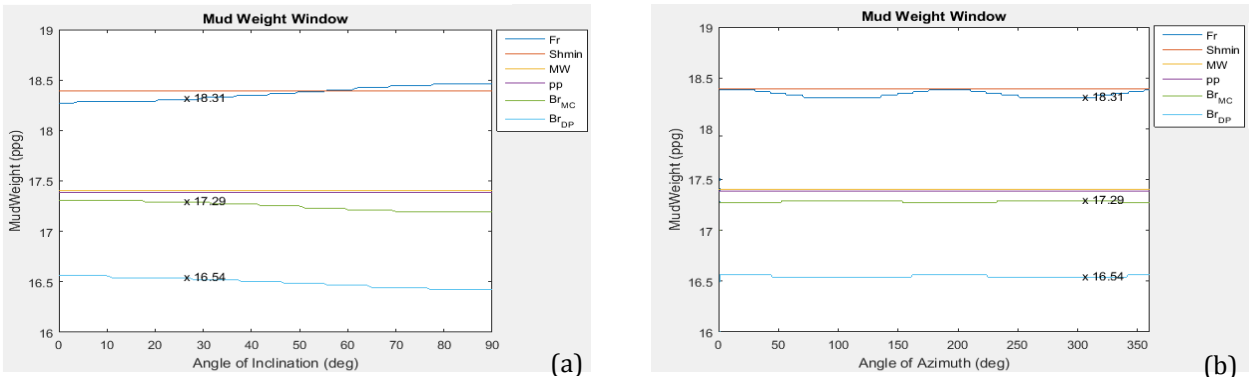

Figure 13. The variation of mud weight as a function of the inclination (a) and azimuth, (b) at 3,053.6 mTVD.

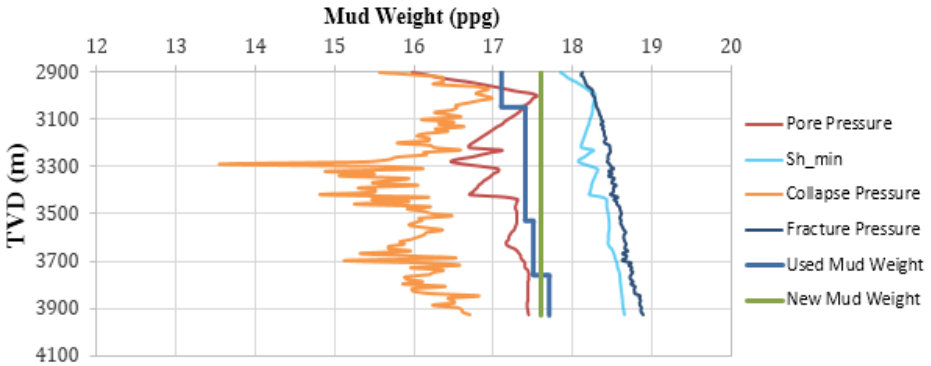

Figure 14. New mud weight program for the drilling section from 2,900 mTVD to 3930 mTVD of the HT-P well.

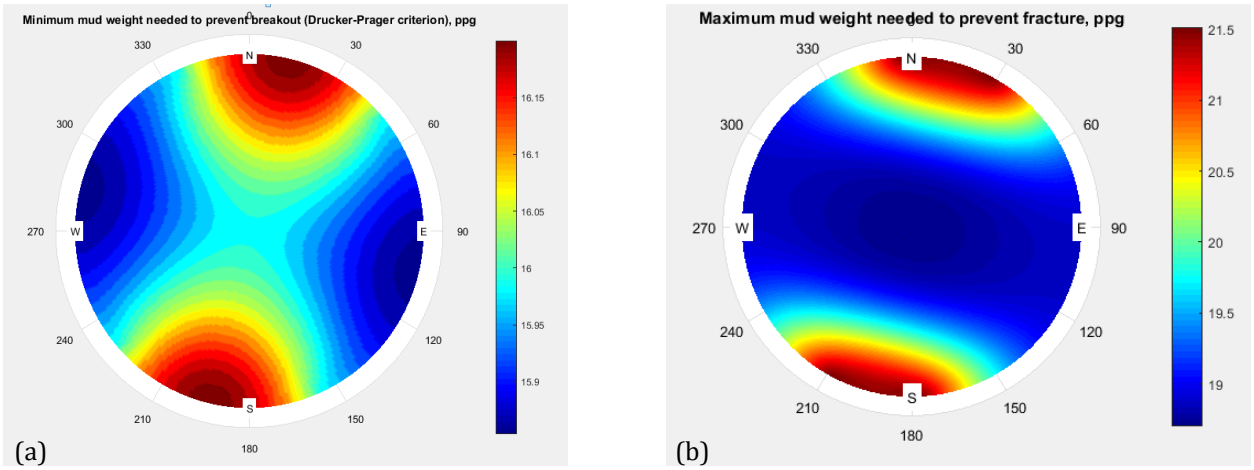

Figure 15. Variation of the mud weight with inclination and azimuth angles at 3,792 mTVD. (a) Minimum mud weight; (b) Maximum mud weight.

The model presented in this study can be used to determine the mud weight for each pair of angles. Figure 15 provides an overview of the variation of the minimum and maximum mud weight as a function of inclination and azimuth angles. The next section will briefly discuss how to read the cloud chart in Figure 15.

Figure 15a shows the minimum mud weight to prevent wellbore collapse and Figure 15b shows the maximum mud weight to prevent fracturing the wellbore. Each point in this cloud chart represents the mud weight for each pair of angles. The distance to the center of the circle is the inclination angle. The center of the circle represents a vertical well and the points along the circumference of the circle represent the wells with inclination angle of 90^o, or horizontal wells. The angle from the North direction (N) to any points in the cloud chart is the azimuth angle of that points. The optimum mud weight for each well should be higher than the value obtained from Figure 15a and lower than the one obtained from Figure 15b. It can be observed that the variation of the mud weight with inclination and azimuth angles is considerable. The collapse pressure of wells drilled along the maximum horizontal stress direction is less than that of the wells drilled along minimum horizontal stress direction (Figure 15a). This means that wells drilled along the maximum horizontal stress direction, especially horizontal wells, need lower mud weight to avoid instability. In addition, it is also easier to hydraulic fracture the wells drilled along the maximum horizontal stress direction ($\theta = 103°$ or $\theta = 283°$) as shown in Figure 15b.

4. Conclusions and Remarks

The high pressure and high temperature condition in the Hai Thach field creates many challenges for drilling operations. This study uses the thermo-chemo-pore-elastic model to calculate the stresses surrounding wellbore and summarizes the petrophysical data to obtain essential input for determining the weight window for HT-P well. The analyses at the troubled zones indicate that the Drucker-Prager criterion provides a better prediction of the collapse pressure than Mohr-Coulomb criterion. A new mud weight of 17.6 ppg is recommended to avoid the risks while drilling the section from 2900 mTVD to 3930 mTVD. In addition, the input data calculated in this study can also be used as a reference for new offset wells drilled in the region. The variation of the optimum mud weight with inclination and azimuth angles is significant for the very narrow mud weight window in this zone. Hence, accurate pressure management while drilling this zone is highly recommended.

Acknowledgement

We would like to acknowledge Bien Dong Petroleum Operating Company (BDPOC) for providing the field data for this study. The first author would like to thank Dr. Son K. Hoang for stimulating discussions during this study.

References

Abousleiman, Y., Hoang, S., and Liu, C. 2013. *Anisotropic Porothermoelastic Solution and Hydro-thermal Effects on Fracture Width in Hydraulic Fracturing*. Int. J. Numer Anal. Met. 38.

Akong, B., Dosunmu, A., Lonna, U., Buduka, S., and Sebastine, M. 2011. *Geomechanical Modeling of Thermal Effects on Wellbore Stability Using the Thermo- Poro-Elastic Model in HPHT Wellbores*. Paper SPE-150771-MS presented at the Nigeria Annual International Conference and Exhibition, Nigeria.

Bui, B. and Tutuncu, A. 2013. *Biot Tensor Approach for Improved Lifecycle Well Integrity*. Paper ARMA-2013-341 presented at the 47th U.S. Rock Mechanics/Geomechanics Symposium, 23-26 June, San Francisco, California, USA.

Ekbote, S. and Abousleiman, Y. 2005. *Porochemothermoelastic Solution for an Inclined Borehole in a Transversely Isotropic Formation*. Journal of Engineering Mechanics.

Hoang, S., Nguyen, S., Khuc, G., Nguyen, D., and Abousleiman, Y. 2016. *Overcoming Wellbore Instability Challenges in HPHT Field with Fully Coupled Poro-Thermo-Elastic Modeling: A Case Study in Hai Thach Field Offshore Vietnam*. Paper OTC-26489-MS presented at the Offshore Technology Conference Asia held in Kuala Lumpur, Malaysia.

Nguyen, S., Hoang, S., Khuc, G., and Tran, H. 2015. *Pore Pressure and Fracture Gradient Prediction for the Challenging High Pressure and High Temperature Well, Hai Thach Field, Block 05-2, Nam Con Son Basin, Offshore Vietnam: A Case Study*. Paper SPE-176276-MS presented at the SPE/IATMI Asia Pacific Oil & Gas Conference and Exhibition, Bali, Indonesia.

Pašić, B., Gaurina-međimurec, N., and Matanović, D. 2007. *Wellbore Instability: Causes and Consequences*. University of Zagreb, Faculty of Mining, Geology and Petroleum Engineering, Pierottijeva 6, 10000 Zagreb, Croatia.

Rasouli, V. and Evans, B., 2010. *Maximised Production through Deviated Drilling and Fracking*. Petroleum exploration society of Australia Resources, 103: 62-64.

Huotari, T. and Kukkonen, I., 2004. *Thermal expansion Properties of Rocks: Literature Survey and Estimation of Thermal Expansion Coefficient for Olkiluoto Mica Gneiss*. Helsinki, Finland: Posiva Oy. Working Report 2004-04.

Wang, Y. and Papamichos, E. 1994. *Conductive Heat Flow and Thermally Induced Fluid Flow around a Wellbore in a Poro-elastic Medium*. Water Resources Research, 30 (12): 3375-3384.

5. Nomenclature

A	Rock constant, dimensionless
B	Rock constant, dimensionless
J_1^{eff}	Octahedral effective normal stress, psi
J_2	Octahedral effective shear stress, psi
σ_m^{eff}	Effective mean stress, psi
R_n	Resistivity at the hydrostatic pressure
T_1	Absolute formation temperature, °C
V_w	Molar volume of water, m^3
a_{df}	Chemical activities of the drilling fluid, dimensionless
a_m	Linear thermal expansion constant, 1/°C
a_{sh}	Chemical activities of shale pore water, dimensionless
k_1	Lithology dependent coefficient
k_2	Lithology dependent coefficient
k_3	Lithology dependent coefficient
k_4	Lithology dependent coefficient
l_m	Reflection coefficient, dimensionless
p_p	Pore pressure, psi
p_w	Bottom hole pressure, psi
v_p	Compressional velocity, m/s
v_s	Shear velocity, m/s
z_w	Water depth, m
ρ_w	Density of seawater, g/cm^3
σ_1	Principal stress, psi
σ_2	Principal stress, psi
σ_3	Principal stress, psi
σ_h	Maximum in-situ horizontal stress, psi
σ_H	Minimum in-situ horizontal stress, psi
σ_{max}	Maximum principle stress, psi
σ_{min}	Minimum principle stress, psi
σ_r	Radial normal stress at wellbore, psi
σ_r^C	Alteration of radial stress due to the osmotic pressure, psi
σ_r^T	Alteration of radial stress due to the thermal induced stress, psi
σ_t	Rock tensile strength, psi

σ_v	Vertical stress, psi
σ_{xx}	Normal stress in x-direction, psi
σ_{yy}	Normal stress in y-direction, psi
σ_z	Axial stress at wellbore, psi
σ_z^C	Osmosis-induced axial stress due to the osmotic pressure, psi
σ_z^T	Thermal-induced axial stress due to the thermal induced stress, psi
σ_{zz}	Axial stress, psi
σ_θ	Hoop stress at wellbore, psi
σ_θ^C	Osmosis-induced hoop stress, psi
σ_θ^T	Thermal-induced hoop stress, psi
τ_{ij}	Shear stress at wellbore, psi
Δt	Measured transit-time, μs/ft
Δt_n	Normal sonic transit time, μs/ft
c	Cohesive strength, psi
d	Radial distance from wellbore axis, m
E	Young´s modulus, psi
g	Gravitational acceleration, m/s^2
I	Well Inclination, degree
n	Eaton exponent, dimensionless
R	Universal gas constant, J/K.mol
r	Wellbore radius, m
R_o	Measured resistivity, Ohm-m
S_v	Overburden stress gradient, psi/ft
T	Circulation temperature, ℃
T_o	Formation temperature, ℃
z	Depth from the sea level, m
α	Biot coefficient, dimensionless
$\Delta\Pi$	Osmotic pressure, psi
ν	Poisson's ration, dimensionless
A_w	Well azimuth, deg.
$\rho(z)$	Bulk density, g/cm^3
φ	Internal friction angle, deg.
ECD	Equivalent Circulation Density
HPHT	High Pressure, High Temperature
PP	Formation Pore Pressure Gradient
PPn	Normal Pore Pressure Gradient
UCS	Unconfined Compressive Strength
XLOT	Extended Leak-off Test